



Published in final edited form as:

Comput Med Imaging Graph. 2011 March ; 35(2): 144–147. doi:10.1016/j.compmedimag.2010.09.005.

Detection of Granularity in Dermoscopy Images of Malignant Melanoma Using Color and Texture Features

William V. Stoecker^a, Mark Wronkiewicz^a, Raed Chowdhury^a, R. Joe Stanley^b, Jin Xu^a, Austin Bangert^b, Bijaya Shrestha^b, David A. Calcara^a, Harold S. Rabinovitz^c, Margaret Oliviero^c, Fatimah Ahmed^d, Lindall A. Perry^e, and Rhett Drugge^f

^aStoecker and Associates, 1702 E. 10th St., Rolla, MO 65401-4600

^bDepartment of Electrical and Computer Engineering, Missouri University of Science and Technology, Rolla, MO 65409-0040

^cSkin and Cancer Associates, 201 N.W. 82nd Avenue, Bennett Medical Plaza, Suite 501, Plantation, FL 33324

^dRolla High School, 900 Bulldog Run, Rolla MO, 65401

^eColumbia Dermatology & Mohs Skin Cancer Surgery, 401 Keene Street, Columbia, MO, 65201

^fSheard & Drugge, PC, 50 Glenbrook Rd Apt 1c, Stamford CT, 06902

Abstract

Granularity, also called peppering and multiple blue-gray dots, is defined as an accumulation of tiny, blue-gray granules in dermoscopy images. Granularity is most closely associated with a diagnosis of malignant melanoma. This study analyzes areas of granularity with color and texture measures to discriminate granularity in melanoma from similar areas in non-melanoma skin lesions.

The granular areas in dermoscopy images of 74 melanomas and 14 melanomas in situ were identified and manually selected. For 200 non-melanoma dermoscopy images, those areas which most closely resembled granularity in color and texture were similarly selected. Ten texture and twenty-two color measures were studied. The texture measures consisted of the average and range of energy, inertia, correlation, inverse difference, and entropy. The color measures consisted of absolute and relative RGB averages, absolute and relative RGB chromaticity averages, absolute and relative G/B averages, CIE X, Y, Z, X/Y, X/Z and Y/Z averages, R variance, and luminance. These measures were calculated for each granular area of the melanomas and the comparable areas in the non-melanoma images.

Receiver operating characteristic (ROC) curve analysis showed that the best separation of melanoma images from non-melanoma images by granular area features was obtained with a combination of color and texture measures. Comparison of ROC results showed greater separation of melanoma from benign lesions using relative color than using absolute color. Statistical analysis showed that the four most significant measures of granularity in melanoma are two color measures and two texture measures averaged over the spots: relative blue, relative green, texture

© 2010 Elsevier Ltd. All rights reserved.

Correspondence should be sent to Dr. Stoecker at The Dermatology Center, wvs@mst.edu, Telephone: 573-364-0122, Fax: 573-364-0129.

Publisher's Disclaimer: This is a PDF file of an unedited manuscript that has been accepted for publication. As a service to our customers we are providing this early version of the manuscript. The manuscript will undergo copyediting, typesetting, and review of the resulting proof before it is published in its final citable form. Please note that during the production process errors may be discovered which could affect the content, and all legal disclaimers that apply to the journal pertain.

correlation, and texture energy range. The best feature set, utilizing texture and relative color measures, achieved an accuracy of 96.4% based on area under the receiver operating characteristic curve.

Index Terms

Melanoma; Image analysis; Texture; Granular; Granularity; Dermoscopy

I. INTRODUCTION

Contact dermoscopy [1] allows detection of granularity, [1,2], which may be seen in images of malignant melanoma. Granularity has been described variously as “granules” [3], “grey-blue to black dust-like dots” [4], “grey-blue pepper-like granules” [3], and multiple, very small, roundish dots of blue-grey color [2]. This feature is better seen with nonpolarized-light contact dermoscopy than with polarized-light dermoscopy [5].

Granularity has been found to be significantly associated with a diagnosis of melanoma, with a sensitivity of 85%, specificity of 99%, and a positive predictive value of 78% [2]. Granular areas can be seen in several types of skin lesions other than melanoma, including lichenoid keratoses. Zaballos et. al. found the granularity pattern in all of the lichenoid keratosis that they examined, however they described it as “diffuse” and “brownish-grey, reddish-brown, bluish-grey or whitishgrey diffuse granules distributed throughout the lesion” [6]. Pastar et al. described a granularity pattern in a regressing seborrheic keratosis [7]. It is also a frequent finding in desmoplastic melanoma, with half of such lesions found to display the feature [8]. Fully regressive melanoma showed regions of granularity in 43% of the lesions studied [9].

The granular, pepper-like appearance of granular areas is a visible form of texture. In dermatology imaging, this research extends texture and color analysis for characterizing semitranslucent areas for skin lesion discrimination [10]. Ten texture co-occurrence matrix characteristics introduced by Haralick et al [11] were examined in this study for analysis of granular areas, including energy average, energy range, inertia average, inertia range, correlation average, correlation range, inverse difference average, inverse difference range, entropy average, and entropy range, which are denoted as T1-T10, respectively. The average and range of these measures in four directions, including 0°, 45°, 90°, and 135°, were calculated using CVIptools [12].

It is the primary purpose of this study to determine if melanoma can be differentiated from other skin lesions by application of color and texture measures from granular areas. The measures chosen are the texture measures defined above and standard color measures determined from the granular areas belonging to melanomas and those areas in non-melanomas which most closely resemble the granular areas in melanomas. A second purpose of this study is to determine which measures, among texture, relative color and absolute color measures, best separate melanoma from other skin lesions.

II. METHODS

The image set used for this study includes contact, non-polarized dermoscopy images [5] of 88 melanomas with granular areas and 200 non-melanoma lesions from four clinics: Skin and Cancer Associates, Plantation, FL, Columbia Dermatology and Skin Cancer, Columbia, MO, Sheard & Drugge, Stamford, CT, and the Dermatology Center, Rolla, MO, selected for dermoscopy study during January–November, 2007. All lesions with any dermoscopy

features of malignancy and any benign lesions for which there was any uncertainty were biopsied. All images were contact, non-polarized dermoscopy images taken with a Sony DSC-W70 7.2 megapixel digital camera with a 3Gen DermLite Fluid dermoscopy attachment (3Gen LLC, San Juan Capistrano, CA).

The 200-image competitive set to which the melanoma set was compared consisted of a variety of lesions encountered in the clinic during the same period in which the melanoma images were acquired. These 200 lesions were both malignant and benign and consisted of a variety of diagnoses: 40 dysplastic nevi, 38 basal cell carcinomas, 21 seborrheic keratoses, 53 nevi (including 13 intradermal nevi, 12 compound congenital nevi, 11 compound nevi, 7 congenital nevi, 5 junctional nevi, 3 acral nevi, 1 compound congenital dysplastic nevus with spitzoid features, and 1 Reed nevus), 8 actinic keratoses, 7 lentiginos, 6 squamous cell carcinomas in-situ, 5 invasive squamous cell carcinomas, 2 benign collision tumors and one collision tumor between a lichen planus like keratosis and squamous cell in-situ, and one between a basal cell carcinoma and seborrheic keratosis, 3 hemangiomas, 2 nevi recurrens, 2 sebaceous hyperplasias, and one from each of 11 other benign lesions.

For the 88 melanomas, a total of 74 invasive melanomas with a median Breslow depth of 0.3 mm and 14 melanomas in-situ, students (JX, DC, and AB) manually marked the most typical granular portion of all images with an approximate oval shape smoothed by a second-order spline. A dermatologist (WVS) adjusted all marked areas as needed. An invasive malignant melanoma with a typical granular area marked is shown in Figure 1. The 200 non-melanoma lesions were manually marked using the same procedure. The areas marked on the non-melanoma lesions were similar in size and as close as possible to the same color and texture as the granular spots in the melanomas. The marked areas in both melanoma and non-melanoma lesions were then analyzed for RGB and chromaticity color features as well as various texture measures based on the co-occurrence matrix.

Color features obtained for all lesions included the following standard measures over the marked spots: average red, green, and blue pixel (R,G,B) values; average relative color (relR, relG, relB) values; average absolute R,G, B chromaticity, where chromaticity in red = $R/(R+G+B)$ and blue and green chromaticity are similarly defined; average G/B, average relG/relB; luminance = $0.30R+0.59G+0.11B$; and variance in R. The relative color values on the spots are defined as $relR = R_{spot} - R_{skin}$, where R_{skin} is the average red color of a small area surrounding the lesion, proportional to the lesion size, and relG and relB are similarly defined [14]. The Commission internationale de l'Eclairage (CIE) trichromatic CIE-XYZ averages [13] for X, Y, Z and ratios X/Y, X/Z and Y/Z for the spots were also calculated, using methods in [10]. Three additional novel relative values calculated were average relative R, G, and B chromaticity, where relative red chromaticity = $relR/(relR+relG+relB)$, and relative blue and green chromaticity are similarly defined. There are nine absolute color features computed over the spot, including the variance in red, average R, average G, average B, average G/B, average R chromaticity, average G chromaticity, average B chromaticity, and average luminance. There are nine relative color features computed over the spot, including the variance in red, average relR, average relG, average relB, average relG/relB, average relR chromaticity, average relB chromaticity, average relG chromaticity, and average luminance.

The ten texture measures and nine color measures, either absolute or relative, were used as inputs to a standard back-propagation neural network implemented in Matlab (MathWorks Inc, Natick MA). The various network architectures used were ten texture and nine absolute or relative color measures, $19 \times 12 \times 6 \times 1$, ten texture measures only, $10 \times 6 \times 4 \times 1$ and nine absolute or relative color measures only, $9 \times 6 \times 4 \times 1$ (4 layers, with 9, 10, or 19 inputs, two hidden layers with 12 and 6 nodes or 6 and 4 nodes in each layer and one output node).

Because of the relatively small data set, a leave-one-out methodology was used for training/test set generation. The neural network was trained up to 15 epochs or until root-mean-square error was less than 0.001. For the granular area data gathered, statistical analysis was performed using SAS software (SAS Corp., Cary, NC) [15].

III. RESULTS

Diagnostic accuracy expressed by the area under the receiver operating characteristic (ROC) curve for detection of melanoma using all 19 texture and relative color measures for granular spots using the back-propagation neural network above, is 0.964. Figures 2 and 3 show the ROC results for the 10 texture features along with the absolute and relative color features, respectively. The vertical and horizontal axes in the ROC curves refer to sensitivity and 1-specificity, respectively, for the ROC curve plots. No improvement was observed with the addition of CIE-XYZ data.

Diagnostic results for different texture pixel distances were compared. Using only the 10 texture measures obtained at pixel distances of 2, 6, and 10, and no color measures, area under the ROC curve was respectively 0.939, 0.958 and 0.946. This optimized pixel distance of 6 gives a texel size of 0.06 mm for granular areas.

Using the SAS Proc Logistic stepwise logistic regression procedure, the measures were selected in the order shown in Table 1. The final model retains five color features, with p-values < 0.0001 for relative green and relative blue over the spots, and six texture features, with p-values 0.0065 for correlation average at a pixel distance of six and 0.0084 for texture energy range. The two relative chromaticity features retained in the logistic regression model, relative green and relative blue chromaticity, are both significant with a p-value = 0.02.

IV. DISCUSSION

The moderately high success rate in separation of melanoma from non-melanoma lesions on the basis of features extracted from granular areas appears promising for early detection of malignant melanoma and warrants pursuit of fully automatic granularity detection. Granularity has a sensitivity for melanoma as high as 85% and a relative risk for melanoma as high as 1.07 [2]. Our ROC analysis indicates that the use of both color and texture measures on granular spots and granular mimics are needed for optimal separation of melanoma from competing diagnoses. In the final model chosen by logistic regression for best melanoma discrimination, there are five color features and six texture features, indicating a significant contribution from both color and texture measures in this model. The most significant of all retained measures were relative blue and relative green colors, with $p < 0.0001$ for both measures. The curves show that diagnostic accuracy as measured by ROC curves is slightly better for relative colors, subtracting background skin color from lesion color, than the results using unmodified absolute color. Relative color was also found to give superior melanoma discrimination in a previous study on blotches in dermoscopy images [16]. Of all ten texture features, correlation average was the most significant texture feature. Correlation average was also the most significant texture feature for discrimination of melanomas from benign lesions using atypical pigment network areas [17].

Our finding of the importance of combining color and texture features to improve discrimination of dermoscopy images confirms other studies on dermoscopy images of pigmented lesions [18,19]. Studies involving other types of images including fiberoptic [20], wound [21], corneal [22], and meat images [23] have also employed combinations of color and texture features. Other studies confirm superior separation by color. For example, one

texture and color-based image retrieval system determined weights for color to be higher than for texture, with red, green, blue, variance and co-occurrence matrix weights respectively 2.4, 2.0, 2.4, 0.8 and 0.9 [17], in agreement with our higher importance for color statistics than texture statistics.

A significant limitation of the study is the use of manual selection of the granular areas. Another limitation is the relatively small number of lesions in the study. A further limitation in the study is the definition of relative chromaticity. If an image has the sum of relative colors $relR+relG+relB$ given in Methods close to zero, the denominator can become vanishingly small, yielding a very large quotient. Replacing the signed quantities with their absolute values yielded worse separation, and the definition of relative chromaticity given in Methods above was retained.

For future work, automatic detection of granular areas will be undertaken using automatic segmentation techniques based on color and texture. In addition, the techniques reported here will be applied to a larger set of lesions.

We made no attempt to select all areas of granularity. Although the presence or absence of granularity (along with other regression structures) is reproducible among experienced dermoscopy practitioners, with an interobserver agreement value $\kappa = 0.44$ determined over 85 lesions [1], it is difficult to reproducibly determine the extent of granularity (Figure 1). We also made no attempt to distinguish “regular granularity” (granules that are homogeneous in size, shape and distribution) from irregular granularity (granules that are heterogeneous in size, shape, distribution and color and associated with white color), which can aid in the differentiation of melanomas from benign lesions [2]. To better accomplish differentiation of granularity in melanomas from granularity in benign lesions, future work could explore the distribution of the granular areas as well as variance in particle size, shape and color in granular areas.

V. CONCLUSION

These results show that granularity in malignant melanomas can be distinguished from similar areas in benign lesions by the application of color and texture measures. The detection of melanoma with a high degree of accuracy and differentiation from a wide variety of lesions, both malignant and benign, is also encouraging, as most studies focus on the more limited problem of discrimination of melanoma from benign pigmented lesions.

Acknowledgments

This publication was made possible by Grant Number SBIR R44 CA-101639-02A2 of the National Institutes of Health (NIH). Its contents are solely the responsibility of the authors and do not necessarily represent the official views of NIH.

References

1. Argenziano G, Soyer HP, Chimenti S, Talamini R, Corona R, Sera F, et al. Dermoscopy of pigmented skin lesions: Results of a consensus meeting via the Internet. *J Am Acad Dermatol.* 2003; 48:679–693. [PubMed: 12734496]
2. Braun RP, Gaide O, Oliviero M, Kopf AW, French LE, Saurat JH, Rabinovitz HS. The significance of multiple blue-grey dots (granularity) for the dermoscopic diagnosis of melanoma. *Br J Dermatol.* 2007; 157:907. [PubMed: 17725673]
3. Zalaudek I, Argenziano G, Ferrara G, Soyer HP, Corona R, Sera F, et al. Clinically equivocal melanocytic skin lesions with features of regression: a dermoscopic-pathological study. *British Journal of Dermatology.* 2004; 150:64. [PubMed: 14746618]

4. Massi D, De Giorgi V, Carli P, Santucci M. Diagnostic significance of the blue hue in dermoscopy of melanocytic lesions: a dermoscopic-pathological study. *Am J Dermatopathol*. 2001; 23:463. [PubMed: 11801781]
5. Benvenuto-Andrade C, Dusza SW, Agero AL, Scope A, Rajadhyaksha M, Halpern AC, Marghoob AA. Differences between polarized light dermoscopy and immersion contact dermoscopy for the evaluation of skin lesions. *Arch Dermatol*. 2007; 143:329. [PubMed: 17372097]
6. Zaballos P, Blazquez S, Puig E, Salsench J, Vives JM, Malveyh J. Dermoscopic pattern of intermediate stage in seborrhoeic keratosis regressing to lichenoid keratosis: report of 24 cases. *British Journal of Dermatology*. 2007; 157:266–272. [PubMed: 17553042]
7. Pastar Z, Lipozencic J, Rados J, Stajminger G. Regressing seborrheic keratosis—clinically and dermoscopically mimicking a regressing melanoma. *Acta Dermatovenerol Croat*. 2007; 15(1):24–26. [PubMed: 17433176]
8. Dabarbieux S, Ronger-Salve S, Dalle S, Balme B, Thomas L. Dermoscopy of desmoplastic melanoma: report of six cases. *British Journal of Dermatology*. 2008; 159:360–363. [PubMed: 18565183]
9. Bories N, Dalle S, Debarieux S, Balme B, Ronger-Salve S, Thomas L. Dermoscopy of fully regressive cutaneous melanoma. *British Journal of Dermatology*. 2008; 158:224–229.
10. Stoecker WV, Gupta K, Shrestha B, Wronkiewicz M, Chowdhury R, Stanley RJ, Xu J, Moss RH, Celebi ME, Rabinovitz HS, Oliviero M, Malters JM, Kolm I. Detection of basal cell carcinoma using color and histogram measures of semitranslucent areas. *Skin Res and Technol*. 2009; 15(3): 283–287. [PubMed: 19624424]
11. Haralick RM, Shanmugam K, Dinstein I. Textural Features for Image Classification. *IEEE Transactions on Systems, Man, and Cybernetics*. 1973; 3(6):610–621.
12. Umbaugh, S. [accessed September 27, 2009] CVIptools, a software package for the exploration of computer vision and image processing. Available at <http://www.ee.siue.edu/CVIptools>
13. Commission internationale de l'Eclairage proceedings. Cambridge UK: Cambridge University Press; 1931.
14. Umbaugh SE, Moss RH, Stoecker WV. Automatic color segmentation of images with application to detection of variegated coloring in skin tumors. *IEEE Eng Med Biol*. 1989; 8(4):43–52.
15. Dilorio, F.; Hardy, KA. *Quick Start to Data Analysis with SAS*. North Scituate Mass: Duxbury Press; 1995.
16. Stoecker WV, Gupta K, Stanley RJ, Moss RH, Shrestha B. Detection of asymmetric blotches (asymmetric structureless areas) in dermoscopy images of malignant melanoma using relative color. *Skin Res Technol*. 2005; 11(3):179–184. [PubMed: 15998328]
17. Shrestha B, Bishop J, Kam K, et al. Detection of atypical texture features in early malignant melanoma. *Skin Res Technol*. 2010; 16(1):60–65. [PubMed: 20384884]
18. Burrioni M, Dell'Eva G, Corona R, Sera F, Bono R, Sbrano P, Andreassi L, Rubegni P. Inter- and intra-variability of pigmented skin lesions: could the ABCD rule be influenced by host characteristics? *Skin Res Technol*. 2004; 10(3):193–199. [PubMed: 15225270]
19. Wollina U, Burrioni M, Torricelli R, Gilardi S, Dell'Eva G, Helm C, Bardey W. Digital dermoscopy in clinical practise: a three-centre analysis. *Skin Res Technol*. 2007; 13(2):133–142. [PubMed: 17374053]
20. Munzenmayer C, Winter C, Rupp S, Kage A, Wittenberg T. Texture-based computer-assisted diagnosis for fiberoptic images. *Conf Proc IEEE Eng Med Biol Soc*. 2009:3735–3738. [PubMed: 19965015]
21. Papazoglou ES, Zubkov L, Mao X, Neidrauer M, Rannou N, Weingarten MS. Image analysis of chronic wounds for determining the surface area. *Wound Repair Regen*. 2010; 18(4):349–358. [PubMed: 20492631]
22. Zhou L, Liu Y, Liu L, Zhuo L, Liang M, Yang F, Ren L, Zhu S. Image analysis on corneal opacity: A novel method to estimate postmortem interval in rabbits. *J Huazhong Univ Sci Technolog Med Sci*. 2010; 30(2):235–239. [PubMed: 20407881]
23. Jackman P, Sun DW, Allen P, Valous NA, Mendoza F, Ward P. Identification of important image features for pork and turkey ham classification using colour and wavelet texture features and genetic selection. *Meat Sci*. 2010; 84(4):711–717. [PubMed: 20374847]

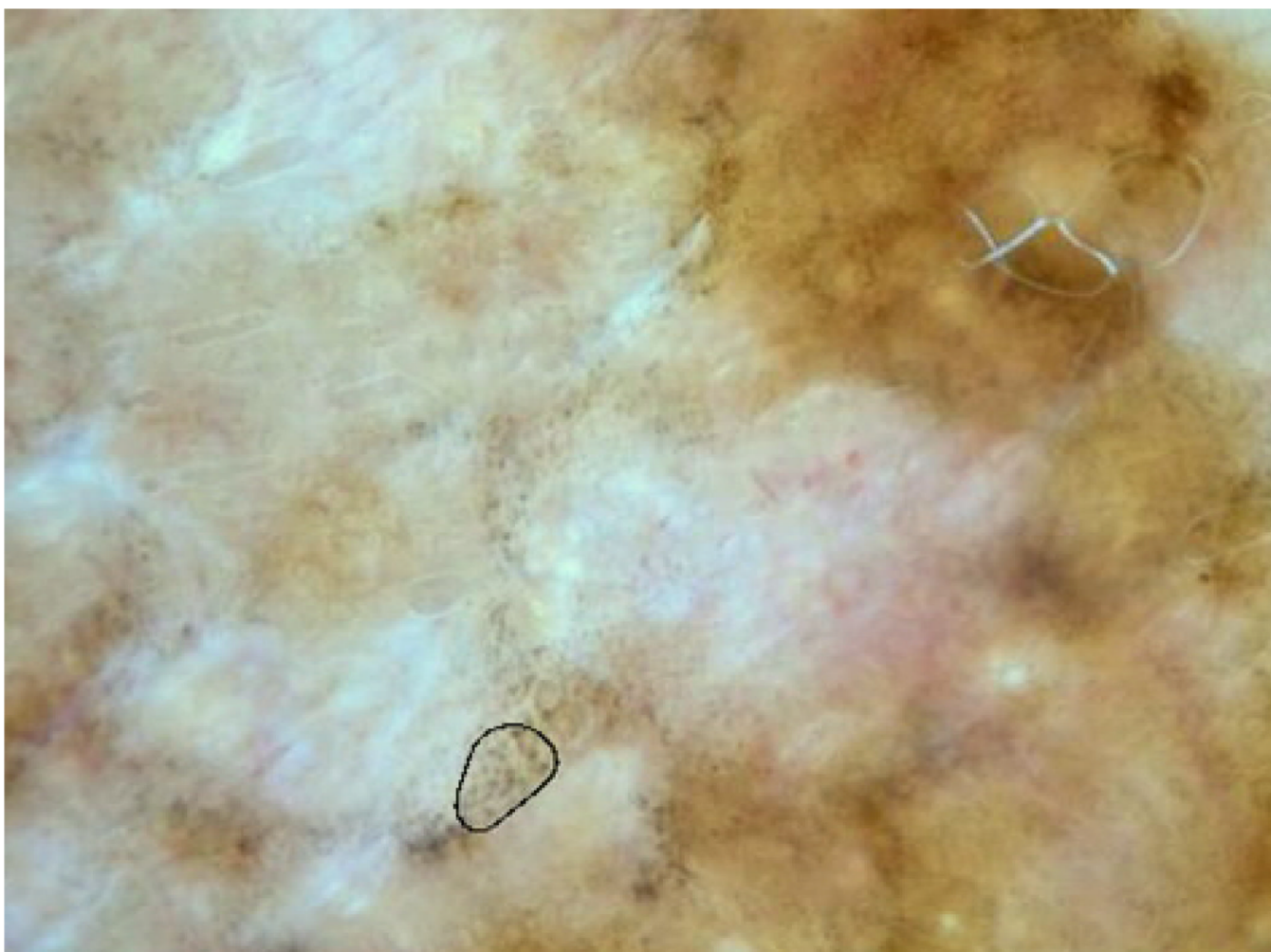


Figure 1. Melanoma with sample granular area marked. The pepper-like granules can be seen in other areas, especially above and to the right of the selected spot.

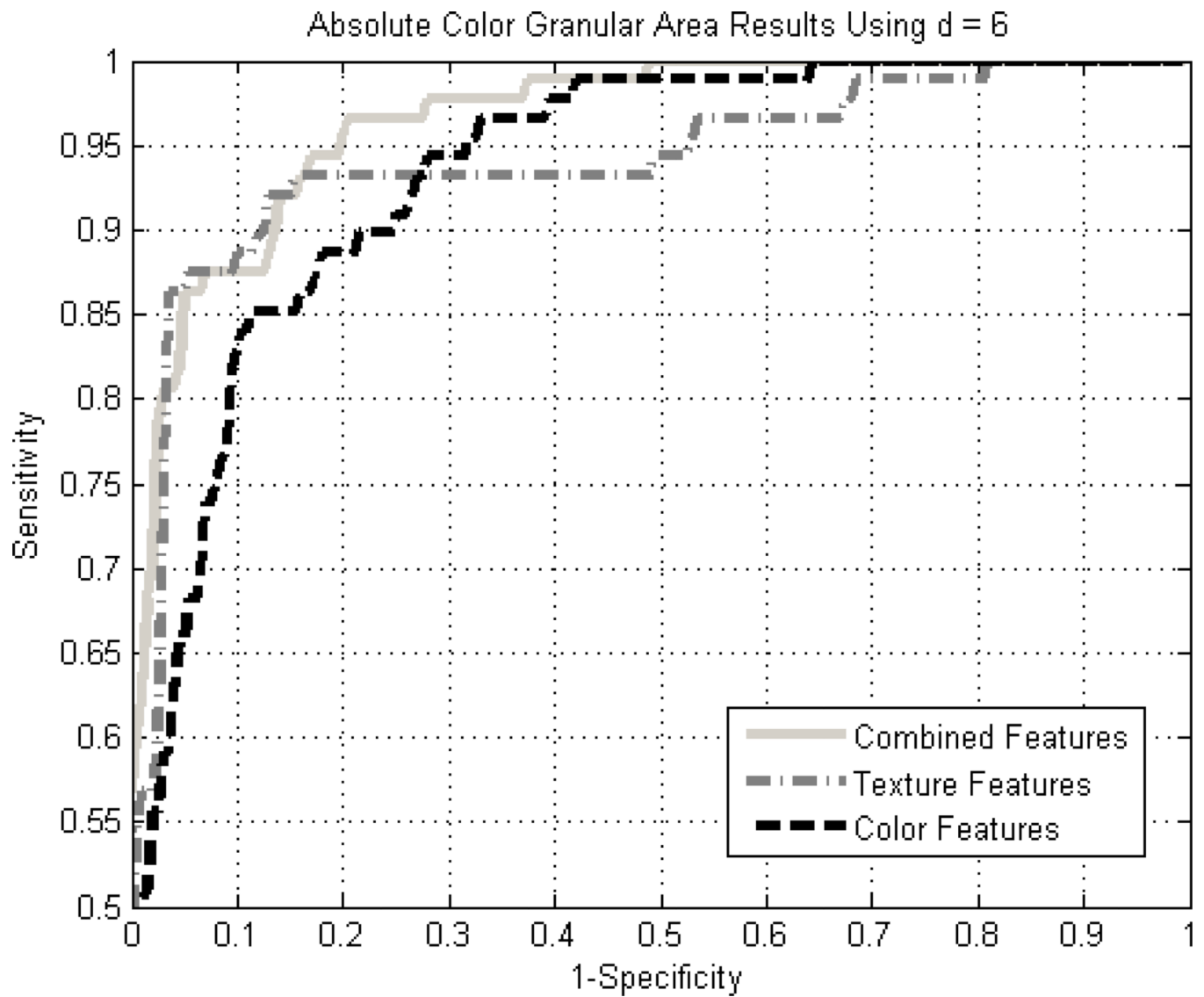


Figure 2. ROC curves for granular results using absolute color for the combined, color-only, and texture-only feature cases using a standard back-propagation neural network with leave-one-out methodology.

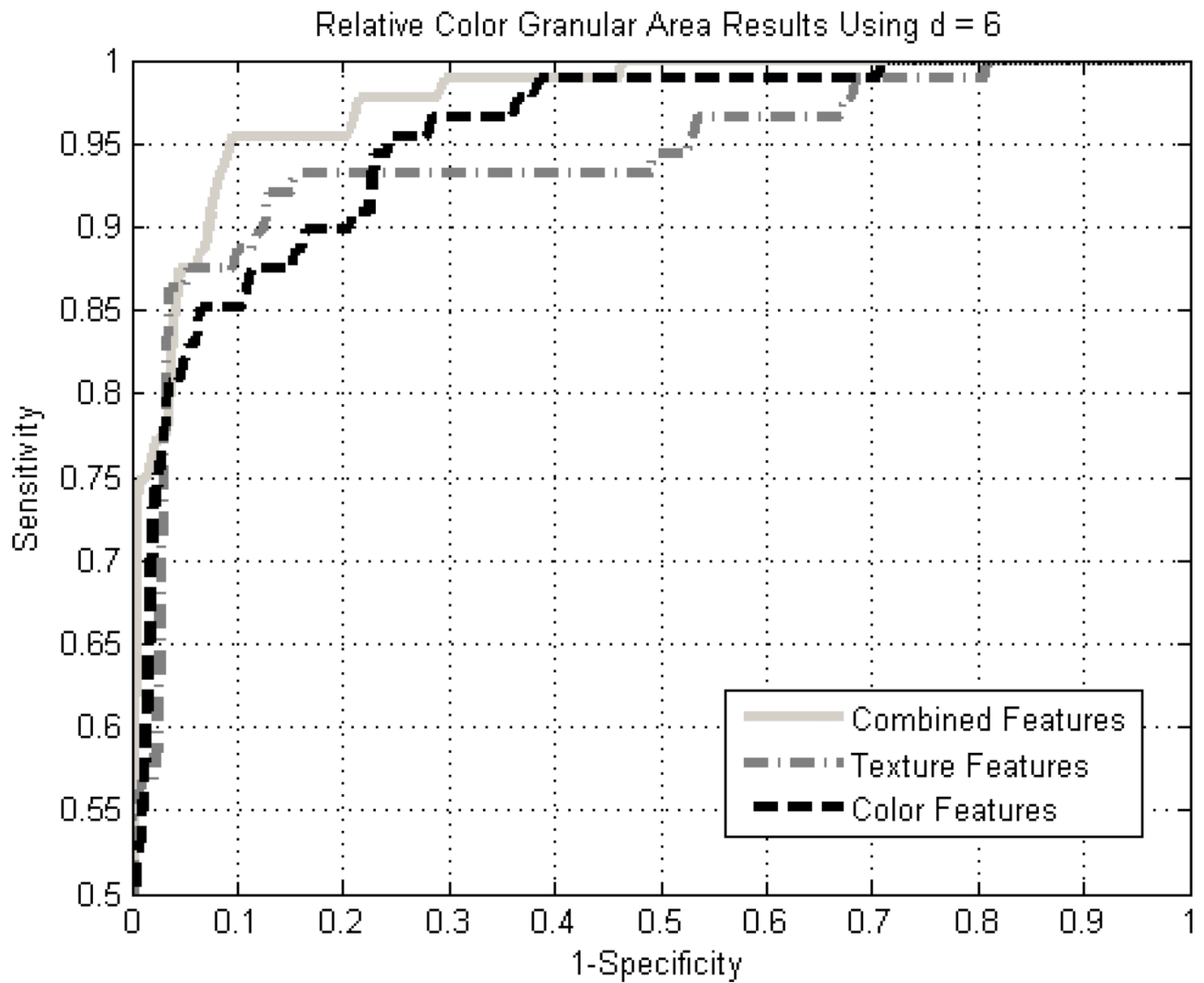


Figure 3. ROC curves for granular results using relative color for the combined, color-only, and texture-only feature cases using a standard back-propagation neural network with leave-one-out methodology.

Table 1

Results of logistic regression procedure, 288 lesions, SAS Proc Logistic, for 19 measures with relative color and texture, pixel distance = 6.

Order of Final 12 features Chosen in SAS Proc Logistic Stepwise Selection in 13 Steps			
Step	Measure	Description (all measures taken over selected spot)	p-values, comments
1	Texture Entropy Average	Average information content of the texture	<0.0001 First measure chosen, highest Chi-sq. score, removed at step 10
2	Relative Blue	Granular area blue minus background blue	<0.0001
3	Relative Green	Granular area green minus background green	<0.0001
4	Texture Entropy Range	Variation of entropy along the four orientations	0.0155
5	Texture Correlation Average	Average measure of similarity between pixels at a specified distance = 6 pixels	0.0065
6	Texture Energy Range	Variation of the homogeneity along the four orientations.	0.0084
7	Relative Green Chromaticity	Relative G / (Rel. R + Rel. G + Rel. B)	0.0203
8	Texture Correlation Range	Variation of correlation along the four orientations	0.1134
9	Red Variance	Variance in red pixel value	0.0997
10	Texture Entropy Average <i>Removed</i>	Average information content of the texture <i>removed</i>	0.6378* 1 st feature selected is now removed from model
11	Texture Inertia Average	Average contrast	0.0218
12	Relative Blue Chromaticity	Relative B / (Rel. R + Rel. G + Rel. B)	0.0210
13	Texture Inertia Range	Variation of contrast along the four orientations	0.1515

p-value, which measures the importance of the variable to the overall model fit, was low for texture entropy average at step 1 but by step 10, this variable no longer contributed significantly to the multivariate model and it was removed.